



Original scientific paper

Tailoring surface properties of functionalized graphene papers aiming to enzyme immobilization

Jéssica Luzardo^{1,2}, Danielle Aguiar¹, Alexander Silva¹, Sanair Oliveira¹, Bráulio Archanjo¹, Renata Simão², Joyce Araujo¹✉

¹Materials Metrology Division, National Institute of Metrology, Quality and Technology (Inmetro), Av. Nossa Senhora das Graças, 50, CEP 25250-020, Duque de Caxias, Brazil

²Nanotechnology Engineering Program - PENt, Federal University of Rio de Janeiro, Av. Athos da Silveira Ramos, 149, Cidade Universitária, CEP 21941-972, Rio de Janeiro, Brazil

Corresponding author: ✉jraujo@inmetro.gov.br; Tel.: +1-111-111-111; Fax: +1-111-111-112

Received: September 3, 2021; Accepted: November 29, 2021; Published: December 15, 2021

Abstract

The use of enzymes as catalysts requires recovery and reuse to make the process viable. Enzymatic immobilization changes enzyme stability, activity, and specificity. It is very important to explore new substrates for immobilization with appropriate composition and structure to improve the efficiency of the immobilized enzymes. This work explores the use of two different graphene oxide papers, one produced by oxidation route (GO) and the other by electrochemical synthesis (EG), aiming for β -galactosidase immobilization. The chemical and structural properties of these two papers were characterized by Raman spectroscopy, X-ray photoelectron spectroscopy and X-ray diffraction. Atomic force microscopy images showed that EG paper ensured more efficient immobilization of the enzymes on the surface of the paper. Cyclic voltammetry was used to monitor the reaction of conversion of lactose to glucose in the free enzyme solution and graphene paper immobilized enzyme solutions. The cyclic voltammetry analysis showed that immobilized enzymes on GO paper showed an improvement in the activity of β -galactose when compared to free enzyme solution, as well as enzyme immobilized on a glassy carbon electrode.

Keywords

Sensors; graphene oxide; β -galactosidase; glucose; lactose; cyclic voltammetry

Introduction

Enzymes are excellent biological catalysts, highly specific, and fundamental in biochemical reactions. They accelerate the speed of reactions without being consumed or modified [1]. Industrially, enzymes have better characteristics than other chemical catalysts due to their higher specificity to the substrate, which promotes the production of only one biochemical reaction and, consequently, allows the synthesis of a specific product with no co-products formation. In addition,

they operate under mild reaction conditions, have a fast action, while the absence of toxicity decreases the environmental and toxicological problems [2]. The use of enzymes as biocatalysts in industries is currently a solution to many problems of modern organic chemistry, which attempts to carry out the most complex reactions under the rules of green chemistry [3]. This is the reason why enzymes are extensively used in the food industry [4-6], biofuels [7-9], textile industry [10-12], pharmaceutical [13-15] and many other industry applications.

β -galactosidase, known as lactase, is an enzyme that has the function of hydrolyzing oligosaccharides, secondary metabolites and D-galactosyl residues of polymers [16]. Lactase is used in industry to improve sweetness, solubility, flavor, and dairy product digestibility. The lactose enzymatic hydrolysis can eliminate serum disposal associated problems, crystallization in frozen concentrated foods and allow milk consumption by lactose-intolerant individuals [17].

Despite unquestionable advantages, there are some practical problems with enzymes, as the high isolation cost, purification, and instability of enzyme structures once they are isolated from their natural environments, sensitivity to process conditions and the presence of substances that may act as inhibitors. Enzymes also work dissolved in aqueous solutions in homogeneous catalysis systems and contaminate the product by hard recovering from the solution in the active state when aiming to posterior reuse [18]. These issues limit their applications in industrial processes and can be solved by enzymatic immobilization on substrates [19]. The use of substrates stabilizes the enzyme's structure, improving its activity. In comparison with free enzymes, immobilized enzymes are more resistant to environmental changes as temperature and pH. It is more important that these systems allow easy recuperation of both enzyme and product, multiple enzyme utilization, continuous operation of enzyme processes, rapid completion of reactions, and a broader range of bioreactor design [18].

β -galactosidase immobilization offers many advantages such as fast reaction, product-controlled formation, easy enzyme removal and adaptability to numerous engineering projects. The reactors containing immobilized β -galactosidases have been extensively studied due to their importance in the industrial production of free lactose milk and whey. Lots of the enzyme reactors used in lactose hydrolysis include papers systems. In a paper bioreactor, the biocatalyst is confined in a well-defined space region by a selective paper or immobilized by adsorption or trapping inside the paper itself. The use of these systems is an effective technique. Both lactose conversion and protein recovery can be performed in one step [17].

The development of nanostructured materials of different sizes and shapes aiming at enzyme immobilization has been investigated as an alternative to the solid bulk substrates [20]. Graphene oxide can be considered the insulating and disordered analog of highly conductive crystalline graphene [21]. The nature of GO is insulating, defective and has a heterogeneous chemical and electronic structure. Its sp^2 hybrid structure, as well as the presence of various types of functional groups containing oxygen at the basal plane and edges, allow GO to interact with a wide range of organic and inorganic materials by non-covalent, covalent and/or ionic bonds interactions, which makes it a promising substrate for multivalent functionalization and efficient loading of small organic molecules and biomacromolecules [1,22]. GO sheets are often an ideal substrate for the study of enzyme immobilization in nanostructured materials. GO sheet contains oxygenated functional groups, making it an ideal substrate for enzyme immobilization without any superficial modifications or any coupling agents [23]. Parvez *et al.* [24] reported a new way of graphene synthesis based on the electrochemical exfoliation of graphite. This method can produce high-quality thin graphene sheets in low reaction times and high yields [25]. In comparison to GO, the graphene oxide produced by this method has a lower oxidation degree and higher defect density caused by the electrochemical process [26,27].

In this work, we prepare two graphene-based papers with different hydrophilicity, GO and EG, aiming to evaluate their efficiency as a support to provide β -galactosidase enzyme immobilization aiming to improve selectivity and activity of this biocatalyst in the reaction of conversion of lactose in glucose and galactose. Surface properties of GO and EG papers were studied by atomic force microscopy (AFM), contact angle and X-ray photoelectron spectroscopy (XPS) measurements. Chemical and structural analysis of graphene papers were evaluated by Raman spectroscopy and X-ray diffraction, respectively, while the morphology was evaluated in a helium ion microscope. The β -galactosidase mediated conversion of lactose in glucose, comparing different immobilization routes, as well as the enzyme in free solution, was evaluated by cyclic voltammetry analysis.

Experimental

Materials

GO synthesis was performed from expanded graphite purchased from Nacional do Grafite Ltda (São Paulo, Brazil). Sodium nitrate (NaNO_3), potassium permanganate (KMnO_4), sulfuric acid (H_2SO_4), hydrochloric acid (HCl) and hydrogen peroxide (H_2O_2) were purchased from Sigma-Aldrich (Missouri, USA). The enzymes used in this work were the commercial samples: Lacday, 10.000 FCC ALU (tablet) and the Deslac Lactose Drops 10.000 FCC ALU. The working electrode was a glassy carbon electrode manufactured by Metrohm, with a working surface diameter of 4 mm.

EG synthesis was performed using a 0.25 mm thickness graphite sheet obtained from Alfa Aesar, Milli-Q water (Millipore system), resistivity $\geq 18 \text{ M}\Omega \text{ cm}^2$. The ammonium sulfate ($(\text{NH}_4)_2\text{SO}_4$) used in the carrier solution was obtained from Sigma-Aldrich (Rio de Janeiro, Brazil). Paper solutions were made from *n, n'*-dimethylformamide (99 %) obtained from Sigma-Aldrich.

Graphene oxide was produced using the modified Hummers methodology [28]. Concentrated H_2SO_4 (92 mL) was added to a mixture of expanded graphite (2.0 g) and NaNO_3 (1.0 g). After the mixture became homogeneous, KMnO_4 (3.0 g) was added slowly. The resulting mixture was then heated to 35 °C and stirred for 30 min. The water (300 mL) was added slowly to the mixture, promoting a highly exothermic reaction and self-heating to 98 °C. External heating was used to maintain the reaction temperature at 98 °C for 15 min and then, the mixture was cooled in an ice bath for 10 min. Afterward, a solution of 10 mL of 30 % v/v H_2O_2 in 90 mL of water was added to stop the exothermic reaction. After the oxidation reaction ceased, a brown suspension was obtained and washed with 180 mL of water and 20 mL of 30 % (v/v) HCl solution to remove metallic ions. Then, a filtration step was performed to separate the non-oxidized graphite. The filtered solution was left to settle for 24 h to remove the acid supernatant. The decanted part corresponding to the graphite oxide was thoroughly washed with water and centrifuged to remove the remaining acid solution. At each wash, the pH of the supernatant was monitored until a neutral value was reached. Residual water was removed using a lyophilization process. The graphite oxide obtained in this step was exfoliated in an ultrasonic bath for 30 min.

Given the challenges regarding large-scale production of large-area defect-free graphene sheets, a new method of graphene synthesis based on the electrochemical exfoliation of graphite has been reported by Parvez *et al.* [24]. Based on this methodology, EG was synthesized by electrochemical exfoliation of graphite using a platinum wire as the counter electrode and a graphite foil as the working electrode. A solution of $(\text{NH}_4)_2\text{SO}_4$ 0.1 mol L^{-1} was used as a carrier electrolyte. The potential of 10 V, applied between the graphite and platinum electrodes, during approximately 30 min, resulted in a complete exfoliation of graphite electrode in the electrolyte. Afterward, EG sheets were separated by electrolyte filtration and dispersed in dimethylformamide (DMF) for 15 min. Four

microliters of EG dispersion (10 mg mL^{-1}) were dropped onto the surface of the glassy carbon electrode and then, the graphene-modified electrode was dried in an oven at $50 \text{ }^\circ\text{C}$ temperature.

GO and EG papers were produced using a vacuum filtration system where the dispersed graphene material was filtered. The paper thickness depends on the concentration and volume of the suspension. For EG papers, 30 mL of 4 mg mL^{-1} of EG solution in DMF were used. For the GO papers preparation, we used 30 mL of a 1 mg mL^{-1} GO solution in water. These solutions were put to filtration using an anodization paper (Anopore Disc) with $0.2 \text{ }\mu\text{m}$ diameter. After complete filtration, the papers were dried in an oven at $60 \text{ }^\circ\text{C}$ until complete drying of adsorbed solvent. During the drying step, the graphene paper detached from the anodizing disk, being easily removed.

The enzyme was immobilized by the adsorption method. For immobilization on the papers, PBS pH 4.5 solutions were prepared using β -galactosidase concentrations of 0.5, 2.0, 5.0 and 10.0 mg mL^{-1} . The solid support (graphene paper) was placed in contact with the enzymatic solution for a period of 30 min under appropriate conditions that favor the enzymatic activity at pH 4.5 and $30 \text{ }^\circ\text{C}$ temperature. The remaining enzyme molecules (not adsorbed) was then removed from the surface by phosphate buffer washing.

Enzyme immobilization on the electrode surface was performed using 9.2 mg enzyme solution in PBS solution at pH 4.5. This solution was placed on the electrode surface and left in an oven at $60 \text{ }^\circ\text{C}$ until the solvent was completely dried. Subsequently, the non-adsorbed enzyme molecules were then removed from the surface by phosphate buffer washing.

Characterization

Contact angle measurements were obtained using a Ramé-Hart, USA, 500 goniometer. Distilled water ($2 \text{ }\mu\text{L}$) was dripped onto EG and GO papers. Measurements were made at different paper positions to verify surface homogeneity. To allow the complete absorption of droplets on the paper surface, they were kept at rest for 1 min.

The atomic force microscope (AFM) (JPK Nanowizard II) was used to investigate the topography of papers before and after enzyme immobilization. Sample images were obtained in intermittent contact mode using a Bruker RTESP cantilever, with a resonant frequency of 273 kHz and an elastic constant of 14 N m^{-1} , determined by Sader's method.

Raman spectroscopic analyzes were performed on a Witec Alpha 300 spectrometer with a 514.5 nm laser line using a $100\times$ objective microscope. Laser power was maintained below 0.1 mW ($<2 \text{ W mm}^{-2}$) to avoid local heat and damage to the samples. All spectra were acquired using 10 s integration time and ten accumulations of 100 to 3600 cm^{-1} . The analyzed spectrum was obtained by the average of five measurements taken at random points to guarantee homogeneity in the results.

X-ray photoelectron spectroscopy (XPS) analyzes were performed in an ultra-high vacuum environment ($p = 10^{-9} \text{ mbar}$) (Scienta Omicron, Germany) using a non-monochromatic X-ray source, Al anode ($K\alpha = 1486.7 \text{ eV}$), with 20 mA emission power and 15 kV voltage. The survey spectra were obtained with 160 eV analyzer step energy and 1 eV acquisition step. High-resolution spectra were collected in the C 1s region with 20 eV analyzer step energy and -0.05 eV acquisition step.

X-ray diffraction (XRD) analyzes were performed on a D8-Focus Bruker diffractometer using Ni-filtered $\text{Cu-K}\alpha$ radiation ($\lambda = 1.5406 \text{ \AA}$) using a scanning interval of 0.02° and 2θ between 5 and 40° . A thin layer of the sample was prepared by ambient drying of the aqueous suspension on Si plates.

Helium ion microscopy (HIM) images were performed by a Zeiss Orion NanoFab, where a focused helium ions beam is used during this analysis, thus eliminating the need for samples coating on conductive metallic thin films. The images were performed at 30 kV and 0.4 pA .

The electrochemical measurements were performed to verify the catalytic activity as well as the selectivity of the immobilized enzyme on graphene, aiming to compare them with the activity and selectivity of free enzymes in solution. Graphene, in this case, was not used in the form of papers as they were not designed to act as a support electrode. Therefore, for the measurements mentioned above, the precursor EG samples were solubilized in DMF (4 mg mL⁻¹) and deposited by casting over printed electrodes to determine the catalytic activity. Cyclic voltammetry measurements were performed using an Autolab potentiostat (PGSTAT 204 model) and NOVA 1.11 software was used for data acquisition. The tests were performed using the three-electrode cell, in PBS pH 7, in the potential range between -1.40 and 0.50 V, step potential of 2.4 mV and step rate of 50 mV s⁻¹. The working electrode used was a carbon screen-printed electrode (CSPE), the counter electrode was a platinum wire, and the reference electrode was the Ag/AgCl electrode in KCl (3 mol L⁻¹). All electro-analytical measurements were performed at room temperature. The presented voltammograms were built from the adjustment of the currents, obtained by subtracting its respective values at the potential of -0.1 V.

The nomenclature of electrodes adopted throughout this work was: carbon screen-printed electrode (CSPE), CSPE with the enzyme immobilized on the surface (CSPE-IE), electrochemically synthesized graphene modified carbon screen-printed electrode (EGPE) and EGPE with the immobilized enzyme on the surface (EGPE-IE). Electrochemical measurements were performed using a lactose solution and glucose (1 mmol L⁻¹) solutions. All conditions tested concerning the condition of the enzyme in the reaction medium, being free solution or immobilized on the electrode surface, are described in Table 1. CSPE-lac and EGPE-lac or CSPE-glic and EGPE-glic correspond to the electrodes in solutions of lactose or glucose respectively, without enzymes in the reaction medium, while CSPE-FE and EGPE-FE correspond to the electrodes with the free enzyme in solution.

Table 1. Nomenclature of tested electrodes

Electrode	Solution	Enzyme	Nomenclature
CSPE	Lactose	No	CSPE-lac
CSPE	Glucose	No	CSPE-glic
CSPE	Lactose	Free	CSPE-FE
CSPE	Lactose	Immobilized	CSPE-IE
EGPE	Lactose	No	EGPE-lac
EGPE	Glucose	No	EGPE-glic
EGPE	Lactose	Free	EGPE-FE
EGPE	Lactose	Immobilized	EGPE-IE

Results and discussion

Morphology analysis (AFM and HIM)

Immobilization was performed at different concentrations, while contact angle measurements and atomic force microscopy were made to verify the presence of enzymes on the paper surface. In this way, it was possible to obtain a qualitative analysis of the distribution of enzymes on the paper surfaces.

Atomic force microscopy (AFM) is one of the micro and nanoscale surface imaging techniques. Due to the direct probe-sample interaction, it is possible to determine certain mechanical, electrical, thermal and optical properties of the material [29]. The AFM was performed to verify the surface characteristics of the produced papers. Figures 1a and 1c show topography images obtained by AFM of EG and GO papers. In these images, one can see typical wrinkles of graphene and some higher

regions (~ 120 nm for both GO and EG), indicating that both papers have regions with different numbers of graphene layers stacked on top of each other. EG is known to have significant heterogeneity and may be more oxidized/exfoliated in some parts than others, and present some non-oxidized/non-exfoliated regions such as the original graphite [26,27]. The topography heterogeneity, as well as different types of defects (edge defects, vacancies, functional groups, heteroatoms) in graphene sheets, mainly generated by the electrochemical oxidation and exfoliation processes, create coordination sites with potential catalysis activity, as the catalytic performance depends on electronic mobility on the surface of materials [30,31].

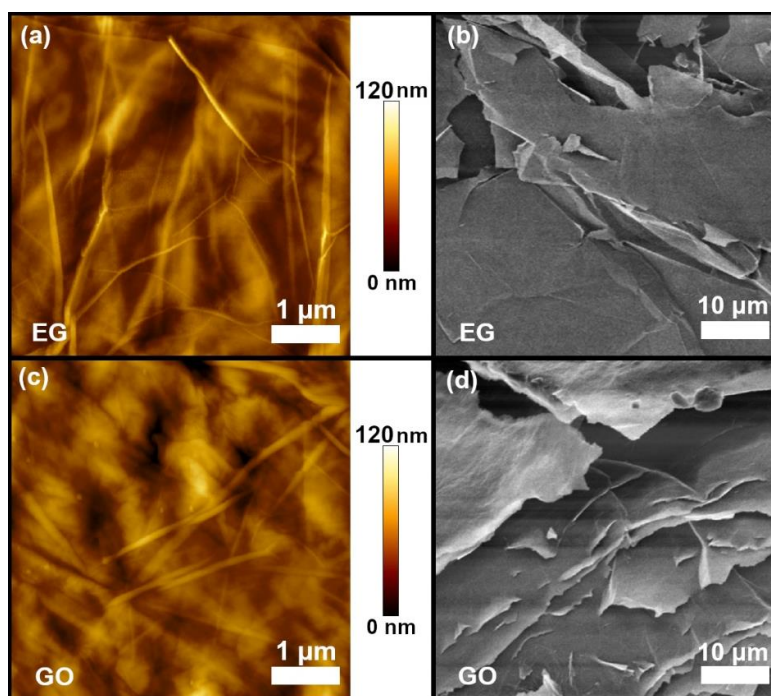


Figure 1. AFM (left) and HIM (right) images of electrochemically produced graphene oxide paper (EG) (a) and (b); chemically produced graphene oxide paper (GO) (c) and (d)

HIM images of EG and GO papers presented in Figures 1b and 1d, show the typical structure of wrinkled graphene sheets before immobilization of the enzymes on the surface. In GO paper (Fig. 1d), it is possible to notice that the sheets are much more compacted, unlike the EG paper structure, where the chemical composition of the surface is much more porous (Fig. 1b). Through cross-section thickness evaluation of two different investigated graphene papers, we found ~ 148 μm for EG paper and ~ 23 μm for GO paper, showing higher compaction in GO paper. The thickness of graphene papers depends on different factors, *i.e.*, chemical forces between carbon layers, as well as the presence or absence of intercalant ions. Hence, the concentration of graphene in the precursor solution is not necessarily proportional to the graphene paper thickness. In the present case, as GO has more intercalant oxygenated functional groups than EG, less material concentration in the solution is needed to form a graphene paper. Besides that, the GO paper morphology has a smaller sheet size than EG paper, which makes sense since the chemical oxidation process causes partial damage in the graphene sheets. This behavior was also observed in the AFM images, which showed a more wrinkled graphene structure for EG than GO paper.

AFM was used to evaluate the presence of enzymes on graphene paper surfaces after immobilization. Through this technique, it was possible to understand how lactases are organized and distributed on the surface of each evaluated paper. Figures 2a-d show the presence of

immobilized enzymes on the EG paper at different concentrations used: 0.5 mg mL⁻¹ (Fig. 2a), 2.0 mg mL⁻¹ (Fig. 2b), 5.0 mg mL⁻¹ (Fig. 2c) and 10.0 mg mL⁻¹ (Fig. 2d). It can be seen that there is a larger number of enzymes in these papers. As the concentration of enzymes in PBS buffer solution increases, they tend to agglomerate, which worsens their distribution on the paper surface.

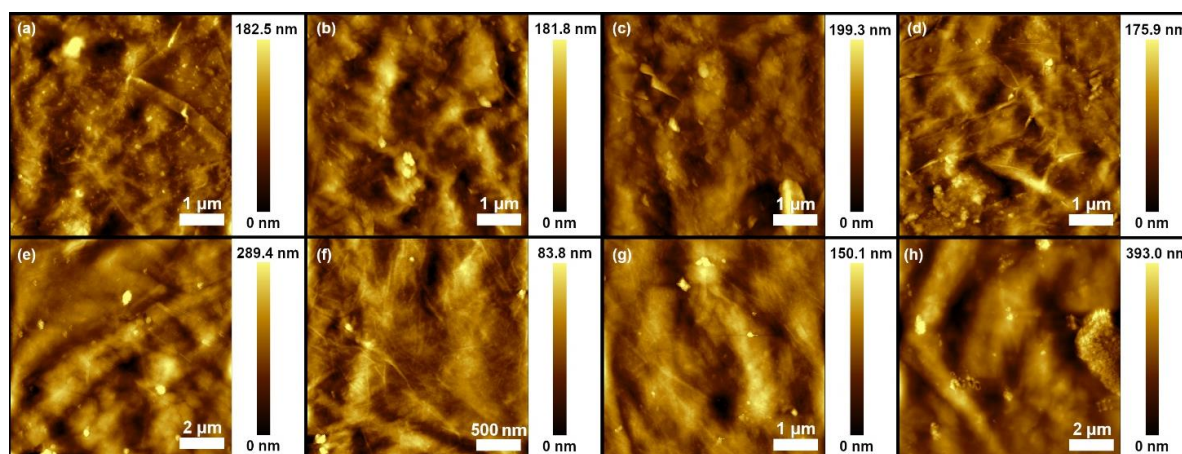


Figure 2. AFM (intermittent contact mode) images of graphene paper surfaces after enzyme immobilization, where EG with β -galactosidase enzymes are shown in: a) 0.5 mg mL⁻¹, b) 2.5 mg mL⁻¹, c) 5.0 mg mL⁻¹ and d) 10.0 mg mL⁻¹, and GO with β -galactosidase enzymes are shown in: e) 0.5 mg mL⁻¹, f) 2.5 mg mL⁻¹, g) 5.0 mg mL⁻¹ and h) 10.0 mg mL⁻¹.

AFM images of GO paper are shown in Figures 2 e-h, for the enzyme concentration of 0.5 mg mL⁻¹ (Fig. 2e), 2.0 mg mL⁻¹ (Fig. 2f), 5.0 mg mL⁻¹ (Fig. 2g) and 10.0 mg mL⁻¹ (Fig. 2h). Observing these images, it is possible to see the presence of enzymes on the surface but in smaller amounts compared to the EG paper. On EG papers, the enzymes are more dispersed, covering the paper surface (small white dots) better, while on GO papers, clusters are formed (large white dots). Since the lateral scale refers to heights, it is possible that in EG samples, these values do not vary so much, which is another evidence that there is a more homogeneous distribution of enzymes over the surface. In GO samples, however, these heights are more inconsistent. This is because there are regions where enzymes are more agglomerated, and these clusters are formed in higher regions in relation to the support.

Consequently, the other regions tend to have smaller heights since most enzymes are not distributed on the surface but present in agglomerates. It is well known that enzymes in aqueous media like PBS buffer keep their hydrophobic sites closed [2,3,20]. However, in the presence of support with a hydrophobic surface, the enzyme opens this active site to adsorb on the support, a mechanism called interfacial activation of the enzyme [32]. EG paper has higher hydrophobicity than GO paper, so it is expected that a larger number of enzymes would adsorb on EG paper surface, as could be seen from the AFM images (Fig. 2). To corroborate this result, water contact angle measurements were performed, and these results will be presented further.

Contact angle measurements

The contact angle was used to verify the wettability of the paper surfaces. Generally, the wettability of a solid surface is strongly influenced by its chemical composition and geometric structure (or surface roughness) and the angle that a drop of water makes with respect to a solid surface shows hydrophilicity or hydrophobicity of a material [33].

Figure 3 shows the water contact angle (WCA) measurements aiming to characterize the surface chemistry of the paper used as a support prior to enzyme immobilization. It was possible to observe that EG paper is less hydrophilic than GO paper due to the higher value of EG paper contact angle

(55.6°). Figures 3a and 3b compare EG paper contact angles with the value found for GO paper (22.9°). The higher hydrophobicity of EG paper is due to the synthesis method. GO paper that was synthesized *via* chemical oxidation route undergoes higher oxidation level than EG paper, which was synthesized *via* electrochemical oxidation route [34].

The WCA measurements were also performed after the enzyme immobilization. In four tested concentration conditions, WCA of EG papers are shown in Figures 3c, 3d, 3e and 3f, while WCA of GO papers are shown in Figures 3g, 3h, 3e and 3f. On these pictures, it was possible to notice significant changes in WCA values after immobilization, especially in the GO paper that before immobilization presented contact angle close to 20° (Fig. 3b), and after immobilization reaches 74.1° (Fig. 3i), in contrast with 55° of WCA of EG paper before immobilization (Fig. 3a) and 79.1° after immobilization (Fig. 3 d).

After the enzyme adsorption, the surfaces of these papers are modified, showing increased hydrophobicity. However, it is believed that with the increase of the enzyme concentration, a particle agglomeration occurs, leading to a poor distribution of the enzymes on the surface, which was already observed. Fig. 3f shows the WCA value for EG paper containing the enzyme in the concentration of 10 mg mL⁻¹, where it is possible to notice that the particle distribution is so heterogeneous that in two measurements performed in different regions of the same surface, in one of them, the drop of water spread completely, and was not possible to measure the contact angle. In the other measurement, the drop presented a WCA of 50.3°. The same effect of heterogeneity was observed for the GO paper, where the highest enzyme concentration shows the lowest WCA value, 21.7° (Fig. 3j). This is supposed to be due to the formation of enzyme clusters because as concentration increases, the dispersion of enzymes becomes less homogeneous.

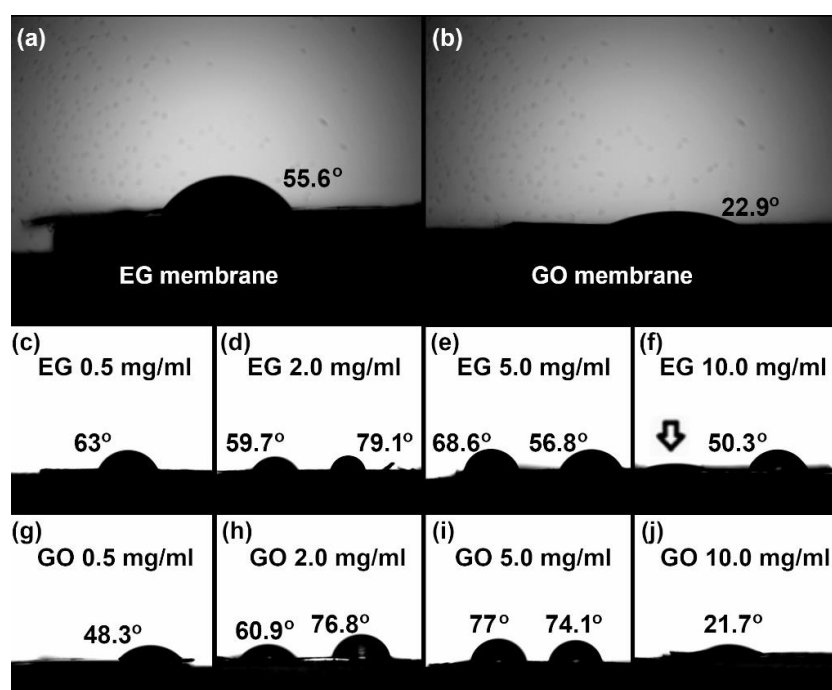


Figure 3. Water contact angle measurements for: EG (a) and GO (b) papers before enzyme immobilization; EG and GO papers with enzymes on the surface in concentrations of: 0.5 mg mL⁻¹ (c) and (g); 2.0 mg mL⁻¹ (d) and (h), 5.0 mg mL⁻¹ (e) and (i); 10.0 mg mL⁻¹ (f) and (j)

Chemical and structural analysis (XPS, Raman and XRD)

XPS analysis provides valuable information on the oxidation level of EG and GO papers. It can qualitatively estimate the percentage of carbon atoms in the basal plane and at the edges of the

graphene sheets. Typically, epoxide, ether, phenol and hydroxyl groups are located at the basal plane, while carbonyl and carboxyl groups are located at the edges [35]. Figures 4a and 4b show XPS spectra of samples in the C1s region.

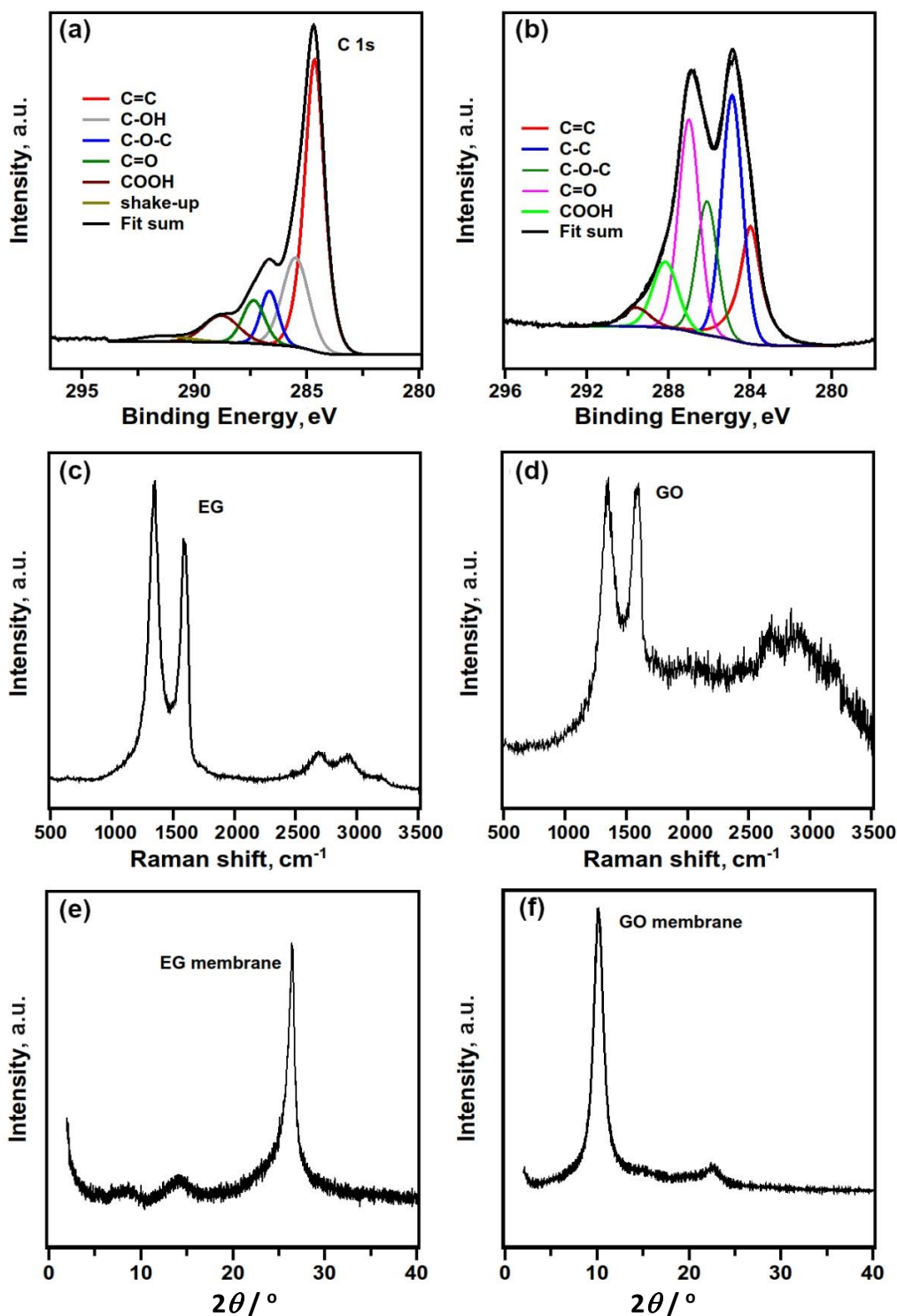


Figure 4. Surface characterization of EG (left) and GO (right) samples: XPS spectra in C1s region (a) and (b); Raman spectra (c) and (d); XRD patterns (e) and (f)

The spectrum for C1s peak was decomposed into six components (Gaussian/Lorentzian function at 70:30 ratio) centered on the following energies: 284.6 eV (sp^2 , C=C bonding of graphite carbon chain), 285.5 eV (sp^3 , C-C bonding of graphite carbon chains) 286.7 eV (C-OH and COC, hydroxyl and epoxy groups, respectively), 287.4 eV (C=O, carbonyl), 288.8 eV (C-OOH, carboxyl) and 291.4 eV

(π - π^* shake-up transition) that is a satellite peak component referring to the interaction of the valence shell electrons with the core electrons) [36]. XPS survey spectra analysis shows that EG paper has a lower oxidation level than a typical graphene oxide material. EG showed the sp^2/sp^3 ratio of ~ 1.5 , while the sp^2/sp^3 ratio for GO was ~ 0.2 . The satellite peak component, called “shake-up,” is a typical feature of delocalized electrons in aromatic systems [36]. This transition is used as an indication of graphitic structure, being present in sp^2 carbon nanomaterials. The presence of π - π^* shake-up satellite peak in C1s spectra of EG sample is due to the preservation of π - sp^2 delocalized electrons, which is absent in GO as the defects generated by the oxidative process in the graphene sheets cause the loss of the delocalization of π - sp^2 electrons [37].

Raman spectra of EG and GO papers are shown in Figures 4c and 4d. G band typically appears at 1580 cm^{-1} , representing the plane elongation of carbon atoms in graphite structure [38-40]. The presence of disorder or defects in the graphene sheets, such as vacancies, oxygen-containing functional groups and/or adsorbed molecules, is revealed by the presence of D-band, centered close to 1350 cm^{-1} [41,42]. The bands centered close to 2700 and 2900 cm^{-1} are known as the second-order contribution of D-band (named 2D) and the combination of G and D bands (named D + G), respectively [43].

The main parameters of D and G bands of EG and GO papers were evaluated from Raman spectra through peak fitting using Lorentzian functions. Table 2 presents the average values of the tuning parameters: frequency (F), FWHM (W) and relative intensity $I(D)/I(G)$. The width of a Raman band may be directly correlated with the disorder degree in a material [44]. The intensity ratio between the C-C stretching (G band) and the defect-induced (D band) modes can be used to measure crystallite sizes (L_a) only for samples with sizes larger than the phonon coherence length, which is found equal to 32 nm. In polycrystalline graphene systems, as the present case, the Raman linewidth of the G band is ideal to characterize the crystallite sizes below the phonon coherence length, down to the average grain boundaries width, which is found to be 2.8 nm. EG sample presented lower G linewidth than GO, Table 2, which indicates higher crystallite size in EG than GO as well as lower defects density, following the model of L_a and L_d described by Cançado *et al.* [40].

Table 2. Mean values of D and G bands evaluated from the Lorentzian peak fitting of Raman spectra of EG and GO samples

Sample	F_D / cm^{-1}	W_D / cm^{-1}	F_G / cm^{-1}	W_G / cm^{-1}	I_D / I_G
EG	1344.1	96.4	1584.5	61.3	0.97
GO	1347.6	126.9	1586.3	80.6	1.12

The XRD pattern of the EG powder sample (Fig. 4e) shows the existence of the characteristic graphite Bragg reflection plane (002), $2\theta = 26.5^\circ$ for $\text{CuK}\alpha$ radiation [46]. This value is equivalent to an interplanar distance around 0.34 nm. The wide peak centered at 26.5° may indicate some layers of graphene stacked in different orientations, as well as different interplanar spaces between them [46]. Castro *et al.* [46] reported that the average lateral size of the initial graphene sheets is inversely correlated with the broadening of the XRD peak. This result reflects that smaller graphene sheets produce more unordered stacking sequences. In the case of the GO paper (Fig. 4f), a single peak in the region of 11° for $\text{CuK}\alpha$ radiation can be seen, equivalent to an interplanar distance of 0.82 nm. This difference between interplanar distances between EG and GO is due to the different oxygen intercalation between graphene sheets promoted by each synthesis process, which is much more intense in the chemical oxidative process than in electrochemical exfoliation. The permeation of oxygenated groups between the graphene sheets is responsible for this increase in the interplanar

distance. In the case of the EG paper, it is possible to notice that there are peaks also at smaller angles, corresponding to larger interplanar distances.

Electrochemical analysis

Previous results (contact angle and AFM images) showed that EG paper exhibited a higher affinity to the enzyme when compared to GO, resulting in more efficient enzyme immobilization. Therefore, EG paper was chosen for catalytic tests aiming to the conversion of lactose into glucose.

Carbon electrodes are commonly used to perform electrochemical experiments. In addition, they have good electrical conductivity, thermal stability and robustness, and are highlighted as the most suitable materials for the design of electrodes with the modified surface [47]. Electrode modification is as a way to add specific physical-chemical properties of the modifying agent to the original electrode, such as enhanced surface area, electrical conductivity, reactivity and selectivity [48].

To check if there was an enzyme action, it is necessary to know the peak position of lactose and some of the reaction products, which is glucose in this case. The voltammetry measurements were performed to detect the conversion of lactose to glucose, mediated by the β -galactosidase enzyme, responsible for the hydrolysis of lactose into glucose and galactose. Two electrodes were tested, a carbon screen-printed electrode (CSPE) and CSPE modified with EG (EGPE). Oxidation peak positions of lactose and glucose analytes at these two electrodes are identified in Table 3.

Table 3. Peak positions of lactose and glucose analytes at CSPE and EGPE

Electrode	Peak potential, V	
	Lactose	Glucose
CSPE	-0.489	-0.375
EGPE	-0.460	-0.337

Knowing the peak positions of lactose and glucose makes it possible to track the catalytic reaction in different enzymatic conditions. The same initial test conditions were maintained for all voltammetry evaluations, with lactose and glucose concentrations of 1 mmol L⁻¹. The lactose and glucose oxidation current peaks measured by cyclic voltammetry at CSPE showed maximums at -0.489 and -0.375 V, respectively, while maximums at EGPE were at -0.460 and -0.337 V, respectively (Table 3).

To understand the role of immobilization on the enzyme activity in this specific reaction of lactose conversion to glucose and galactose, the free enzyme activity was also monitored. Corrected voltammograms (*cf.* Experimental part) for CSPE are shown in Figure 5a, where it can be seen that when the enzyme is placed free in a solution containing lactose (green curve), there was a decrease in the lactose peak intensity compared to the response in solution without enzyme (red curve). This indicates a suppression in the lactose content in the solution, while a small shift of the oxidation peak (from -0.489 to -0.463 V) towards the glucose potential (-0.375 V) suggests that lactose hydrolysis is probably happening. This solution was stored, and a new measurement was performed after 48 hours. In the voltammetry experiment recorded in the solution containing the free enzyme after 48 h of reaction (orange curve), the peak appears centered at -0.395 V, referring to the glucose potential. The presence of this new peak and the absence of the lactose peak suggests that the enzyme present in the solution continued to perform its function of converting lactose into glucose. After 48 hours, all lactose has been converted and that is why the peak position was changed to glucose potential.

The voltammetric responses evaluated with the EGPE electrode under different conditions of enzyme immobilization are shown in Figure 5b. The curve for the EGPE-FE sample represents the condition when the enzyme is placed free in solution (green curve), and this voltammogram showed

the oxidation peak at -0.337 V referring to glucose oxidation, and no peak in the lactose region at -0.46 V (red curve). This shows that the conversion was efficient as there was no change in the peak height after 48 h of reaction (orange curve). When the enzyme is not immobilized but free in solution, its structure would not be stabilized to expose its active sites, which explains the low intensity observed. This is because even free in solution, the enzyme interacts with the electrode surfaces of CSPE and EGPE. The better interaction between the graphene at the EGPE electrode surface with the enzyme's hydrophobic sites promotes the enzyme's stabilization since, in a biological environment, enzymes are typically linked to cellular structures aiming to their stabilization.

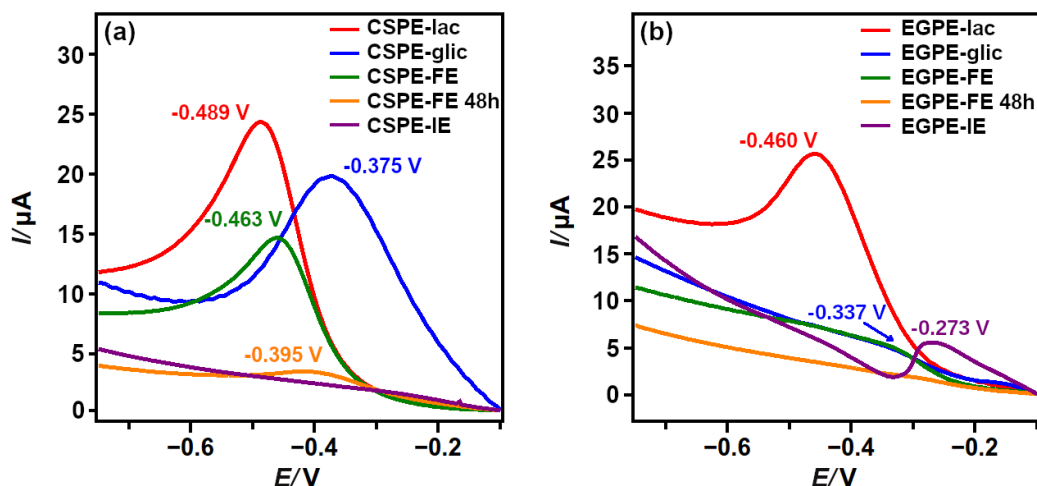


Figure 5. Normalized voltammograms of CSPE (a) and EGPE (b) in: pure lactose solution (red), pure glucose solution (blue), lactose solution with free enzyme (green), lactose solution with free enzyme after 48 h of reaction (orange) and lactose with immobilized enzyme (purple)

By comparing voltammograms of the enzyme immobilized on two electrodes, CSPE and EGPE, it was possible to observe that for CSPE-IE (purple curve), no peak was detected, probably due to a poor chemical interaction between hydrophobic sites of the enzymes and CSPE electrode surface. It is reasonable to assume that the enzyme's active site, responsible for the hydrolysis of the lactose to glucose, was inactivated by the linkage of the enzyme with CSPE support, annulling the catalytic power of the enzyme. All modifications and measurements with the developed biosensors were done under strictly identical conditions. As expected, the reduction signal was improved when EG was present. Using EGPE-IE, it is possible to see that the conversion happens instantly with the appearance of the glucose peak at -0.273 V, corroborating the idea that EG improves the catalytic power of the β -galactosidase enzyme in the conversion reaction of lactose to glucose. As already discussed, enzymes interact with EG through their hydrophobic sites. When free in an aqueous solution, the enzyme tends to close its active sites due to the more hydrophilic environment. This process ends up interfering with the conversion reaction of lactose into glucose. In the EGPE-FE system, the enzymes that effectively participated in the conversion process were close to the surface of the modified electrode, which could interact with the surface and expose their active sites. Thus, there is an increase in the glucose signal as soon as the electrode is placed in the solution since all electrode deposited enzymes have their active sites exposed and are prepared to start the conversion as soon as they come into contact with lactose. The glucose potential shift observed in the EGPE-IE electrode voltammogram (Fig. 5b, purple curve) is due to the higher energetic barrier in the reaction of conversion of lactose to glucose in the presence of the immobilized enzyme than in the case of free enzyme since the mobility of charge carriers is lower at the electrode surface (EGPE-IE) than in electrolyte solution. The mobility of electrolyte ions is reduced in solid-state as the

graphene paper electrode surface, increasing the activation energy to convert lactose to glucose. Consequently, the voltammetric peak is shifted from 0,337 V to 0,273 V, as observed in Figure 5b.

Conclusions

In this work, the synthesis of graphene papers was performed by two different routes: chemical synthesis and electrochemical exfoliation. The immobilization of the β -galactosidase enzyme was carried out on two synthesized papers having different surface chemical properties, EG (more hydrophobic) and GO (more hydrophilic). The enzyme immobilization efficiency was dependent on the hydrophilicity of papers and the concentration of enzymes in the electrolyte solution. Higher catalysis efficiency was observed when the EG paper was chosen as the support. Compared to GO paper, EG paper has more hydrophobic active sites, which are preferentially available to interact with the hydrophobic sites of enzymes. In addition, it was observed that high enzyme concentration in the solution is unfavorable since it promotes enzyme agglomeration and, consequently, a poor distribution over the substrate.

Cyclic voltammetry evaluation shows that graphene oxide produced by electrochemical exfoliation is the better substrate for immobilization. The electrochemical tests showed improved results for the EGPE electrode in comparison with the CSPE electrode. The immobilized enzyme on the EGPE electrode showed instantaneous lactose to glucose conversion reaction, with the appearance of the glucose peak at -0.273 V, corroborating the idea that EG improves the catalytic power of the β -galactosidase enzyme. This result could be explained by considering that EG functional groups at the basal plane and edges of graphene defects help electron transfer to the redox sites of the enzymes, favoring the detection of products by the electrodes. In addition, the method used was adsorption to the substrate, which allows the enzyme to immobilize in a more energetically favorable way, stabilizing its structure and assisting in its activity.

Acknowledgement: The authors would like to acknowledge BITS Pilani, Hyderabad and Council for Scientific and Industrial Research, CSIR Grant No: (No:22/0784/19/EMR II), which helped us in publishing this article.

References

- [1] L. Jin, K. Yang, K. Yao, S. Zhang, H. Tao, S.-T. Lee, Z. Liu, R. Peng, *ACS Nano* **6** (2012) 4864-4875. <https://doi.org/10.1021/nn300217z>
- [2] M. A. Z. Coelho, A. M. Salgado, B. D. Ribeiro, *Enzimatic Technology (tradução: Tecnologia Enzimática)*, EPUB, Rio de Janeiro, Brazil, 2008, p. 288. ISBN 978-85-87098-83-2 (In Portuguese)
- [3] R. Fernandez-Lafuente, *Molecules (Basel, Switzerland)* **22**(4) (2017) 601. <https://doi.org/10.3390/molecules22040601>
- [4] C. D. Grande, J. Mangadlao, J. Fan, A. De Leon, J. Delgado-Ospina, J. G. Rojas, D. F. Rodrigues, R. Advincola, *Macromolecular Symposia* **374** (2017) 1600114. <https://doi.org/10.1002/masy.201600114>
- [5] F. Li, H.-Y. Yu, Y.-Y. Wang, Y. Zhou, H. Zhang, J.-M. Yao, S. Y. H. Abdalkarim, K. C. Tam, *Journal of Agricultural and Food Chemistry* **67** (2019) 10954-10967. <https://doi.org/10.1021/acs.jafc.9b03110>
- [6] F. Ning, T. Qiu, Q. Wang, H. Peng, Y. Li, X. Wu, Z. Zhang, L. Chen, H. Xiong, *Food Chemistry* **221** (2017) 1797-1804. <https://doi.org/10.1016/j.foodchem.2016.10.101>
- [7] M. M. Antunes, P. A. Russo, P. V. Wiper, J. M. Veiga, M. Pillinger, L. Mafra, D. V. Evtuguin, N. Pinna, A. A. Valente, *ChemSusChem* **7** (2014) 804-812. <https://doi.org/10.1002/cssc.201301149>

- [8] I. Beenish, M. I. Ahamed, A. M. Asiri, K. A. AlAmry, *Materials Science for Energy Technologies* **1** (2018) 63-69. <https://doi.org/10.1016/j.mset.2018.03.003>
- [9] K. Guan, Q. Liu, Y. Ji, M. Zhang, Y. Wu, J. Zhao, G. Liu, W. Jin, *ChemSusChem* **11** (2018) 2315-2320. <https://doi.org/10.1002/cssc.201800479>
- [10] R. Jalili, S.H. Aboutalebi, D. Esrafilzadeh, R. L. Shepherd, J. Chen, S. Aminorroaya-Yamini, K. Konstantinov, A. I. Minett, J. M. Razal, G. G. Wallace, *Adv. Funct. Mater.* **23** (2013) 5345-5354. <https://doi.org/10.1002/adfm.201300765>
- [11] N. D. Tissera, R. N. Wijesena, J. R. Perera, K. M. N. de Silva, G. A. J. Amaratunge, *Applied Surface Science* **324** (2015) 455-463. <https://doi.org/10.1016/j.apsusc.2014.10.148>
- [12] Y.J. Yun, W.G. Hong, W.-J. Kim, Y. Jun, B.H. Kim, *Adv. Mater.* **25** (2013) 5701-5705. <https://doi.org/10.1002/adma.201303225>
- [13] J. Liu, L. Cui, D. Losic, *Acta Biomater.* **9** (2013) 9243-9257. <https://doi.org/10.1016/j.actbio.2013.08.016>
- [14] V. K. Rana, M.-C. Choi, J.-Y. Kong, G. Y. Kim, M. J. Kim, S.-H. Kim, S. Mishra, R. P. Singh, C.-S. Ha, *Macromolecular Materials and Engineering* **296** (2011) 131-140. <https://doi.org/10.1002/ma.me.201000307>
- [15] X. Sun, Z. Liu, K. Welsher, J. T. Robinson, A. Goodwin, S. Zaric, H. Dai, *Nano Research* **1** (2008) 203-212. <https://doi.org/10.1007/s12274-008-8021-8>
- [16] A. S. Godoy, Structural and functional studies of bacterial beta-galactosidase enzymes (tradução: Estudos estruturais e funcionais das enzimas beta-galactosidasas de bactérias), Doctoral Thesis, Physical Institute, University of São Paulo, São Carlos (2016). <https://doi.org/10.11606/T.76.2017.tde-04012017-145940>
- [17] Q. Husain, *Crit. Rev. Biotechnol.* **30** (2010) 41-62. <https://doi.org/10.3109/07388550903330497>
- [18] B. Krajewska, *Enzyme Microb. Technol.* **35** (2004) 126-139. <https://doi.org/10.1016/j.enzmictec.2003.12.013>
- [19] J. Fan, J. Luo, Y. Wan, *J. Membr. Sci.* **538** (2017) 68-76. <https://doi.org/10.1016/j.memsci.2017.05.053>
- [20] D. Kishore, M. Talat, O. N. Srivastava, A. M. Kayastha, *PloS One* **7** (2012) e40708. <https://doi.org/10.1371/journal.pone.0040708>
- [21] S. C. Ray, *Applications of graphene and graphene-oxide based nanomaterials*, Elsevier Science, 2015, p. 39-55. <https://doi.org/10.1016/C2014-0-02615-9>
- [22] K. Parvez, Z.-S. Wu, R. Li, X. Liu, R. Graf, X. Feng, K. Müllen, *Journal of the American Chemical Society* **136** (2014) 6083-6091. <https://doi.org/10.1021/ja5017156>
- [23] S. Lim, J. H. Han, H. W. Kang, J. U. Lee, W. Lee, *Carbon Letters* **30** (2020) 409-416. <https://doi.org/10.1007/s42823-019-00110-3>
- [24] S. M. Oliveira, J. M. Luzardo, L. A. Silva, D. C. Aguiar, C. A. Senna, R. Verdan, A. Kuznetsov, T. L. Vasconcelos, B. S. Archanjo, C. A. Achete, E. D'Elia, J. R. Araujo, *Thin Solid Films* **699** (2020) 137875. <https://doi.org/10.1016/j.tsf.2020.137875>
- [25] L. A. Silva, J. M. M. Luzardo, S. M. Oliveira, R. V. Curti, A. M. Silva, R. Valaski, R. B. Capaz, J. R. Araujo, *Current Applied Physics* **20** (2020) 846-852. <https://doi.org/10.1016/j.cap.2020.04.004>
- [26] J. Zhang, F. Zhang, H. Yang, X. Huang, H. Liu, J. Zhang, S. Guo, *Langmuir* **26** (2010) 6083-6085. <https://doi.org/10.1021/la904014z>
- [27] K. P. Loh, Q. Bao, G. Eda, M. Chhowalla, *Nature Chemistry* **2** (2010) 1015. <https://doi.org/10.1038/nchem.907>
- [28] W. S. Hummers, R. E. Offeman, *Journal of the American Chemical Society* **80** (1958) 1339-1339. <https://doi.org/10.1021/ja01539a017>
- [29] A. Sikora, M. Woszczyzna, M. Friedemann, F. J. Ahlers, M. Kalbac, *Micron* **43** (2012) 479-486. <https://doi.org/10.1016/j.micron.2011.11.010>

- [30] X. Fan, *Frontiers in Materials* **1** (2015). <https://doi.org/10.3389/fmats.2014.00039>
- [31] X. Zuo, S. He, D. Li, C. Peng, Q. Huang, S. Song, C. Fan, *Langmuir* **26** (2010) 1936-1939. <https://doi.org/10.1021/la902496u>
- [32] A. M. Brzozowski, U. Derewenda, Z. S. Derewenda, G. G. Dodson, D. M. Lawson, J. P. Turkenburg, F. Bjorkling, B. Høge-Jensen, S. A. Patkar, L. Thim, *Nature* **351** (1991) 491-494. <https://doi.org/10.1038/351491a0>
- [33] J. Rafiee, M. A. Rafiee, Z.-Z. Yu, N. Koratkar, *Adv. Mater.* **22** (2010) 2151-2154. <https://doi.org/10.1002/adma.200903696>
- [34] P. Kumar, *International Journal of Engineering Trends and Technology* **49** (2017) 128-136. <https://doi.org/10.14445/22315381/IJETT-V49P220>
- [35] S. Park, R. S. Ruoff, *Nat. Nanotechnol.* **4** (2009) 217. <https://doi.org/10.1038/nnano.2009.58>
- [36] J. Araujo, A. Silva, C. Gouvêa, E. S. Lopes, R. A. A. Santos, L. Terrazos, R. Capaz, C. A. Achete, I. Maciel, *Carbon* **99** (2016) 1-7. <https://doi.org/10.1016/j.carbon.2015.11.059>
- [37] K. L. S. Castro, R. V. Curti, J. R. Araujo, S. M. Landi, E. H. M. Ferreira, R. S. Neves, A. Kuznetsov, L. A. Sena, B. S. Archanjo, C. A. Achete, *Thin Solid Films* **610** (2016) 10-18. <https://doi.org/10.1016/j.tsf.2016.04.042>
- [38] A. Kaniyoor, R. Sundara, *AIP Advances* **2** (2012) 032183. <https://doi.org/10.1063/1.4756995>
- [39] K. Krishnamoorthy, G. S. Kim, S. J. Kim, *Ultrason. Sonochem.* **20** (2013) 644-649. <https://doi.org/10.1016/j.ultsonch.2012.09.007>
- [40] J. Ribeiro-Soares, *Carbon* **95** (2015) 646-652. <https://doi.org/10.1016/j.carbon.2015.08.020>
- [41] L. G. Cançado, A. Jorio, E. H. M. Ferreira, F. Stavale, C. A. Achete, R. B. Capaz, M. V. O. Moutinho, A. Lombardo, T. S. Kulmala, A. C. Ferrari, *Nano Letters* **11** (2011) 3190-3196. <https://doi.org/10.1021/nl201432g>
- [42] R. Saito, M. Hofmann, G. Dresselhaus, A. Jorio, M. S. Dresselhaus, *Advances in Physics* **60** (2011) 413-550. <https://doi.org/10.1080/00018732.2011.582251>
- [43] M. E. Mendoza, E. H. M. Ferreira, A. Kuznetsov, C. A. Achete, J. Aumanen, P. Myllyperkiö, A. Johansson, M. Pettersson, B. S. Archanjo, *Carbon* **143** (2019) 720-727. <https://doi.org/10.1016/j.carbon.2018.11.070>
- [44] E. H. Martins Ferreira, M. V. O. Moutinho, F. Stavale, M. M. Lucchese, R. B. Capaz, C. A. Achete, A. Jorio, *Physical Review B* **82** (2010) 125429. <https://doi.org/10.1103/PhysRevB.82.125429>
- [45] A. C. Ferrari, J. Robertson, *Physical Review B* **61** (2000) 14095-14107. <https://doi.org/10.1103/PhysRevB.61.14095>
- [46] K. Castro, S. Oliveira, R. Curti, J. Araújo, L. Sassi, C. Almeida, E. Ferreira, B. Archanjo, M. Cabral, A. Kuznetsov, Electrochemical response of glassy carbon electrodes modified using graphene sheets of different sizes. *Int. J. Electrochem. Sci.* **13** (2018) 71-87. <http://doi.org/10.20964/2018.01.02>
- [47] H. Maleki, C. D. Cojocar, C. M. A. Brett, G. M. Jenkins, J. R. Selman, *JEIS* **145** (1998) 721-730. <https://doi.org/10.1149/1.1838337>
- [48] P. R. Moses, L. Wier, R. W. Murray, *Analytical Chemistry* **47** (1975) 1882-1886. <https://doi.org/10.1021/ac60362a043>

